Stable Vacancy Clusters in Neutron-Irradiated Graphite: Evidence for Aggregations with a Magic Number

Z. Tang,[1] M. Hasegawa,[1,2] T. Shimamura,[2] Y. Nagai,[2] T. Chiba,[3] Y. Kawazoe,[1] M. Takenaka,[4] E. Kuramoto,[4] and T. Iwata[5]

[1]*Institute for Materials Research, Tohoku University, Sendai 980-8577 Japan*
[2]*The Oarai Branch, Institute for Materials Research, Tohoku University, Oarai, Ibaraki 311-1313, Japan*
[3]*National Institute for Research in Inorganic Materials, Tsukuba 305-0044, Japan*
[4]*Research Institute for Applied Mechanics, Kyushu University, Kasuga, Fukuoka 816-8580, Japan*
[5]*Japan Atomic Energy Research Institute, Tokai, Ibaraki 319-1195, Japan*

(Received 12 June 1998)

By combining positron-annihilation experiments and first-principles calculations, abundant planar V_6 rings are identified in heavily neutron-irradiated graphite. The calculations show that the V_6 ring is particularly stable. Annealing experiments exhibit that the V_6 ring survives up to 1500 °C. These results suggest vacancies aggregating with the magic number in graphite. [S0031-9007(99)08756-6]

PACS numbers: 61.72.Ji, 61.80.–x, 78.70.Bj

Vacancy-type defects (vacancy and n-vacancy aggregation V_n) have crucial effects on various properties of the host materials and thus have been intensively studied. However, the nature of the V_n clusters, for instance, those in semiconductors generated during crystal growth and during device fabrication by dry ething or by radiation-based techniques, is still unclear to a large extent [1–3]. Corbett and Bourgoin [1] suggested puckered V_6 ring in the diamond-structure lattice, since the six-membered ring is the closed building block in this lattice. Chadi and Chang [2] predicted that the V_6 ring and the V_{10} cage closed by four V_6 rings in silicon (sp^3 hybrid) are particularly stable (namely, they are magic vacancy clusters V_n with the magic numbers $n = 6$ and 10), which is supported by a successive first-principles calculation [4]. However, the magic V_n clusters, expected as the particularly stable forms of defects, are not yet well evident *experimentally* due to the difficulties in identification of vacancy clusters.

In this Letter, we discuss an interesting example in graphite, a technologically (as nuclear material) and scientifically (as a prototypical sp^2 hybrid) important material [5,6]. The planar six-membered ring is the closed structural unit of various (sp^2 covalent) carbon materials, such as graphite, nanotubes, fullerenes, etc. [6]. It is thus expected that the planar V_6 rings have high stability in these systems. We here investigate the nature of irradiation-induced defects in graphite. Abundant planar V_6 rings, which are the smallest magic vacancy clusters as shown by our first-principles calculations, are indeed found in a heavily neutron-irradiated graphite. The present study provides evidence for the magic vacancy aggregations for the first time.

The experimental method used in this work is the positron annihilation technique (PAT). Its unique capability for defect study is originated from the fact that positrons are sensitively trapped at the defects and are annihilated there with the surrounding electrons [7]. Recent studies have shown that experiment complemented by calculation can reveal microscopic structural features of defects [3,8–11]. We here focus on the positron one-dimensional (1D) angular correlation of annihilation radiation (ACAR) distribution and the positron lifetime for defect-free (bulk), electron-irradiated, and neutron-irradiated highly oriented pyrolytic graphite (HOPG). The experiments are compared with first-principles calculations based on the newly developed two-component density-functional (TCDF) theory [8,9]. The irradiation-induced defects are then identified based on these comparisons.

In the experiments, the HOPG samples (ZYA grade, Union Carbide Co.) were irradiated with 3 MeV electrons to 1.0×10^{18} e/cm^2 [2.5×10^{-5} displacements per atom (dpa)] below 50 °C (labeled by "E"), and with fast neutrons ($E > 1$ MeV) to 1.4×10^{20} n/cm^{-2} (0.20 dpa) at 60 °C (labeled by "N"), respectively. The positron 1D-ACAR and lifetime measurements were performed at room temperature (general descriptions for the experiments can be found in our previous paper [12]). The ACAR measurements yield a 1D-ACAR distribution proportional to the projection of the three-dimensional momentum density (3D-MD) [$\rho(\mathbf{p})$] of the positron-electron pair on a selected axis p_z. The results of the p_z along the crystallographic direction [0001] (i.e., the $p_{\|c}$ direction perpendicular to the basal plane) are presented in this Letter.

The 1D-ACAR for the bulk [unirradiated (U)] shows a marked bimodality with two peaks around $p_{\|c} = \pm 3.1$ mrad (Fig. 1a) [13,14]. The peak ratio defined as the peak height relative to the momentum density at $p_{\|c} = 0$ is evaluated to be 1.20. After the electron irradiation (E), the bimodality is found to be much suppressed (Fig. 1a). It is noteworthy that this 1D-ACAR includes a small contribution of the positron annihilation in the bulk as indicated by the lifetime result (Table I).

 0031-9007/99/82(12)/2532(4)$15.00

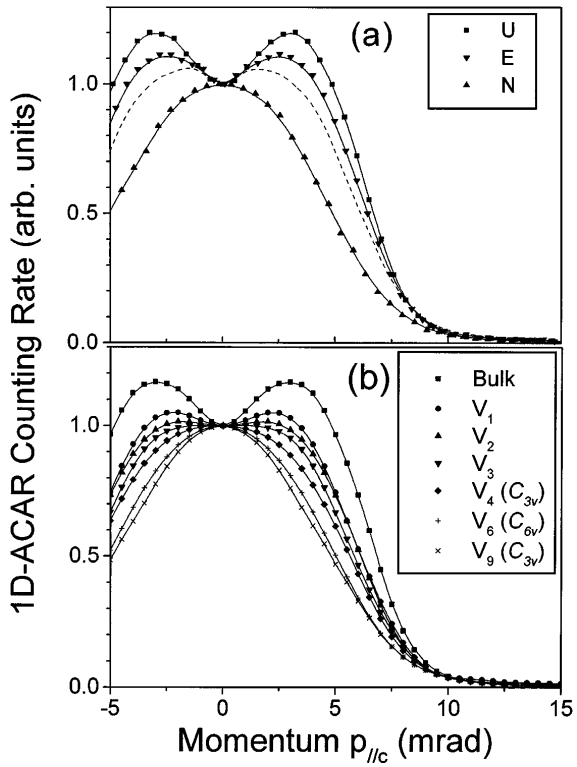

FIG. 1. (a) Experimental 1D-ACAR distributions for the unirradiated (U), electron-irradiated (E), and neutron-irradiated (N) graphites; the full defect component in E is shown by the dashed line. (b) Calculated distributions (after convoluted with a correction function for a finite detector length) for the bulk and various planar V_n clusters.

After decomposing the 1D-ACAR to the bulk (U) and the defect components using a positron trapping model [15], we find that the peak ratio of the *full* defect 1D-ACAR (Fig. 1a) reduces to 1.06 while the peak positions shift toward the center (at ± 1.7 mrad). More dramatically, after the heavy neutron irradiation (N) the bimodality disappears *completely* and only a central peak (at $p_{\|c} = 0$) is observed (Fig. 1a). On the other hand, the positron lifetimes at the defects are found to increase from 233 ps (E) to 350 ps (N) (Table I).

To understand the experiments, we calculate the 3D-MD and the lifetime (τ) based on the TCDF theory within the local density approximation (LDA) [8,9]. The recent LDA scheme given by Puska *et al.* [9] is adopted. The plane waves with the maximum kinetic energy of 600 eV are employed as the basis set. The 96-site supercell is used for simulating the defects in the crystal and the Brillouin-zone integration is performed using three special k points for the electrons [16] and the Γ point for the positron. Details of the method were previously described [11].

TABLE I. Experimental positron lifetimes for the samples.

Sample	Irradiation	τ_1 (ps)	τ_2 (ps)	I_2 (%)
U	unirrad.	210 ± 0.2	···	···
E	e^-	121 ± 10.4	233 ± 1.5	91 ± 1.5
N	n	···	350 ± 0.3	99 ± 1.6

Figure 1b shows the calculated 1D-ACAR distributions for the bulk and various planar V_n clusters. The calculations are found to well reproduce the experiments: The peak ratio and the peak positions of the calculated bimodality for the bulk (Fig. 1b) are 1.17 and ± 2.9 mrad, respectively, in good agreement with the experimental values (1.20 and ± 3.1 mrad). Moreover, the shape of the defect 1D-ACAR is found to vary from a suppressed bimodality for the monovacancy to a narrow central peak for the large V_n clusters (Fig. 1b): In the V_1 case, the peak ratio (positions) reduces (shift) to 1.05 (± 2.1 mrad); in the cases of V_2 and V_3, the 1D-ACAR distributions in the low-momentum region become almost flat; in the cases of large V_n clusters having high symmetries [namely, V_4 (C_{3v}), V_6 (C_{6v}), and V_9 (C_{3v}) in Fig. 2], the calculations show only a central peak and the peak becomes narrower when the cluster size becomes larger. On the other hand, the calculated positron lifetime is found to increase from 209 ps for the bulk to 378 ps for the V_9 (C_{3v}) [17] (Fig. 2).

The calculations indicate that these notably characteristic 1D-ACAR distributions and lifetimes are originated from the positron density distribution (PDD). To understand this origin, we plot the calculated bulk 3D-MD distribution on the $[2\bar{1}\bar{1}0]$ plane through the Γ point in Fig. 3a (those in whole momentum space can be approximated by a rotation of this distribution around the p_z ([0001]) axis by omitting a small hexagonal anisotropy). The dominant reason for the bimodality is the double peaks of the 3D-MD centered at $p_z \sim \pm 4$ mrad on the p_z axis, which are further decomposed band-by-band in Fig. 4. It is clear that the peak is mainly contributed from an enhanced p_z atomic momentum wave function (AMWF) of the π bands, while the contribution from

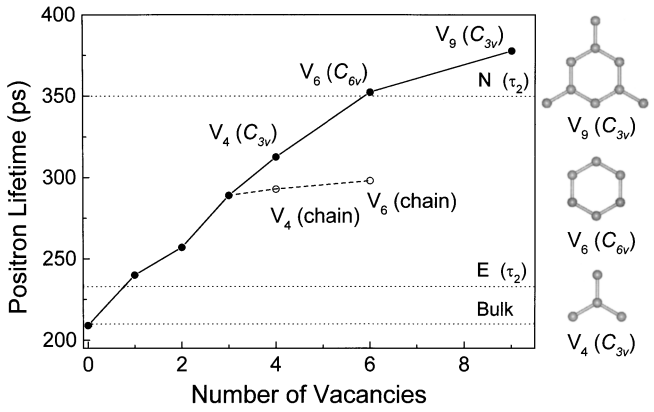

FIG. 2. Calculated positron lifetimes for the bulk and planar V_n clusters in graphite. Structures of some V_n are shown on the right together with *plane* symmetries of vacant sites. The experimental positron lifetimes are indicated by thin horizontal dashed lines.

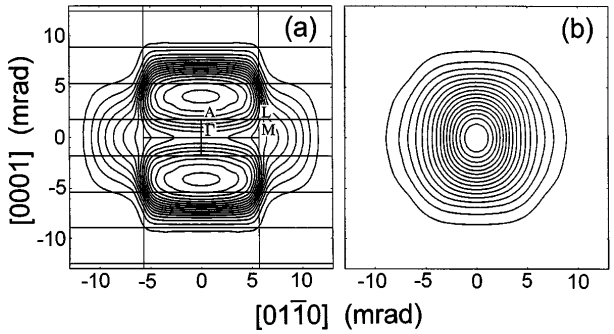

FIG. 3. Calculated 3D-MD distributions at the [2$\bar{1}\bar{1}$0] plane through the Γ point for (a) the graphite bulk and (b) the V_6 (C_{6v}). The contour spacing is $\frac{1}{16}$ of the maximum. The intersections of the Brillouin zones with this plane are indicated by thin lines in (a).

an s AMWF of the σ bands (sp^2 hybrid bonds) is suppressed because of the quasi-two-dimensional (QTD) PDD in the bulk (which has maxima between the basal planes and significantly samples the p_z orbitals).

In the cases of positron trapped at the *planar* defects, with the increase of the defect size the PDD progressively loses this QTD characteristic (Fig. 5), and its maximum transfers from the interplanes to the defect center in the plane. As a result, the p_z AMWF contribution to the 3D-MD progressively reduces to be negligible (Fig. 3b) and a rather *s*-like characteristic, namely, the narrow central peak in both the 3D-MD and 1D-ACAR for the V_4 (C_{3v}), V_6 (C_{6v}), and V_9 (C_{3v}) is thus expected. Moreover, we find that a further increase of the number of the vacancies in a zigzag chain more than three (V_3) does not lead to an obviously deeper positron trapping since the potential well perpendicular to the chain direction is similar. As a result, the positron lifetime is almost the same for the V_n (chain) ($n \geq 3$) (Fig. 2) and the 1D-ACAR distributions for the V_4 (chain) and V_6 (chain) are found to be only slightly narrower than that for the V_3.

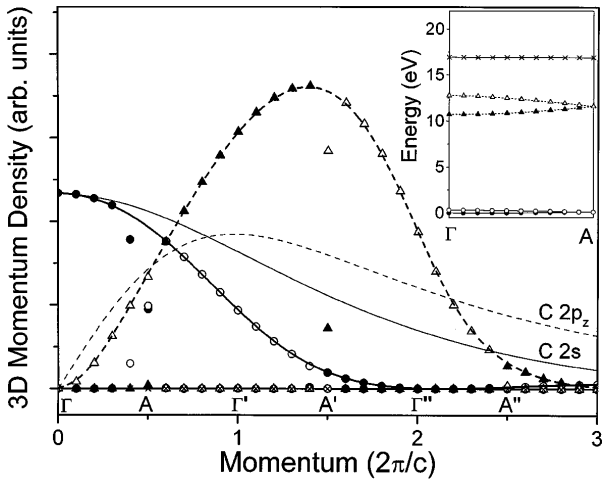

FIG. 4. Decomposed theoretical 3D-MD along the p_z ([0001]) axis for the graphite bulk. The band structure along this direction is shown in the inset. The σ (π) bands are indicated by solid (dashed) lines. The carbon $2s$ ($2p_z$) atomic momentum wave function is shown by the thin solid (dashed) line.

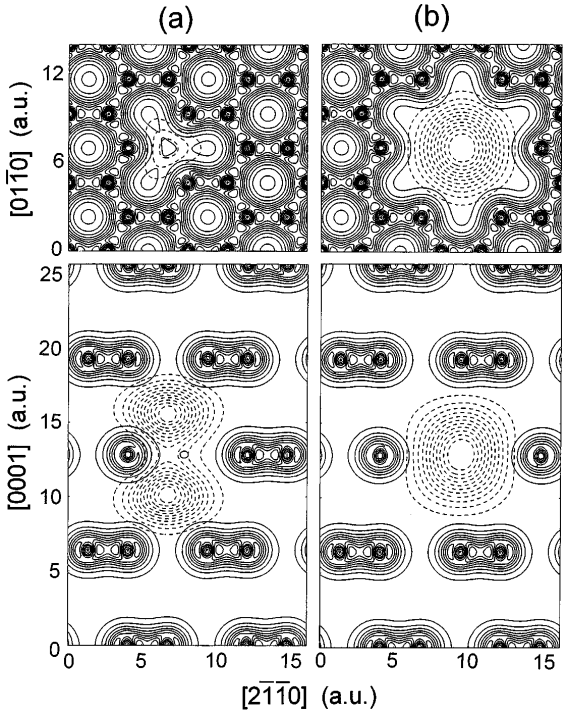

FIG. 5. Electron (solid lines) and positron (dashed lines) densities in the basal and hexagonal prism planes of graphite through the defect center for (a) the V_1 and (b) V_6 (C_{6v}). The contour spacing of solid (dashed) lines is $3.5 \times 10^{-2} e^-/a_0^3$ ($8.7 \times 10^{-4} e^+/a_0^3$).

We now identify the irradiation-induced defects by comparing the experiments with the calculations. The calculations indicate the defects in the electron-irradiated sample (E) to be the monovacancies, since the calculated bimodal peak ratio (1.05) and positron lifetime (240 ps) for the monovacancies (Figs. 1b and 2) agree well with the experiments (1.06 and 233 ± 2 ps) (Fig. 1a and Table I). This is consistent with the fact that 3 MeV electron irradiation around room temperature induces mostly monovacancies [5].

For the neutron-irradiated sample (N), only one defect-lifetime component is well extracted. As indicated by further annealing experiments (Table II), this lifetime can be attributed to a dominant lifetime about 365 ± 8 ps

TABLE II. Annealing behaviors of the defect lifetime components for the neutron-irradiated sample (N).

T (°C)	τ_2 (ps)	τ_3 (ps)	I_2 (%)	I_3 (%)
1100	245 ± 15.6	364 ± 5.7	26 ± 6.4	73 ± 6.3
1300	243 ± 14.8	364 ± 10.7	46 ± 8.3	50 ± 9.0
1500	222 ± 8.2	367 ± 8.0	54 ± 3.8	42 ± 4.5

(averaged) mixed with other shorter ones with only very small intensities [18]. The calculations indicate the defects to be mainly the planar V_6 (C_{6v}) rings, because *both* the calculated full width at half maximum (which can characterize a central peak) of the 1D-ACAR (5.06 mrad) (Fig. 1b) and the calculated lifetime (352 ps) (Fig. 2) agree well with the experiments (4.90 mrad and 365 ± 8 ps) (Fig. 1a and Tables I and II).

Finally, we discuss why there exist abundant V_6 (C_{6v}) rings after the heavy neutron irradiation. We calculate the formation energy E_f for various V_n with optimized geometries. It is found that the averaged formation energy of a sp^2 dangling bond is about 2.3 eV, and the formation energy of the V_n is approximated by $E_f = 2.3 \times N_{\mathrm{DB}}$ eV [here N_{DB} is the number of sp^2 dangling bonds but a rather weak binding of the π-π bonds is omitted]. N_{DB} is equal to $n + 2$ for the V_n (chain), while closing a chain to form a ring reduces the value of N_{DB} and, consequently, results in a minimum in the averaged vacancy formation energy (E_f/n). The V_6 (C_{6v}) ($N_{\mathrm{DB}} = 6$) is just the smallest cluster of a closed ring, namely, the smallest magic vacancy cluster. [The calculated E_f/n for the V_1, V_6 (C_{6v}), and V_n (chain) is 6.91, 2.35, and about $(2.3 + \frac{4.6}{n})$ eV, respectively.] This indicates the formation of the V_6 ring to be energetically favorable and stable. During the irradiation, vacancy clusters and monovacancies of high densities are produced in collisional cascades. Those monovacancies will get enough energy to migrate shortly during local lattice agitation by subsequent irradiation to grow the vacancy clusters to the stable V_6 rings. The annealing experiments exhibit rather V_6 rings surviving and no further vacancy aggregating with them even up to 1500 °C (Table II). In the electron irradiation, however, rather isolated monovacancies are induced in so low density that they will annihilate at some sinks but have effectively no opportunity to coalesce to higher multivacancies during the irradiation and even annealing at high temperature.

In conclusion, the vacancy-type defects in irradiated graphites are studied experimentally and theoretically using the PAT. The stable vacancy clusters in the heavily neutron-irradiated graphite are identified to be planar V_6 rings, the smallest magic vacancy clusters with a high stability as shown by the calculations. Since the closed (planar or puckered) sixfold rings of bonds are the basic structural units in a variety of covalently bonded materials, such as carbon nanotubes, fullerenes, elemental semiconductors, SiC, etc., the present study indicates that the V_6 rings will have particular stabilities in these materials.

We thank M. Narui and M. Yamazaki at the Oarai Branch, and H. Sunaga and H. Takizawa at the JAERI-Takasaki Institute, for their electron irradiation under the Inter-University program of the University of Tokyo. This work is partly supported by a Grant-in-Aid for Scientific Research of the Ministry of Education, Science and Culture (No. 10450229).

[1] J. W. Corbett and J. C. Bourgoin, in *Point Defects in Solids*, edited by J. H. Crawford, Jr. and L. M. Slifkin (Plenum, New York, 1975), Vol. 2, p. 1.
[2] D. J. Chadi and K. J. Chang, Phys. Rev. B **38**, 1523 (1988).
[3] M. Saito and A. Oshiyama, Phys. Rev. B **53**, 7810 (1996).
[4] A. Oshiyama, M. Saito, and O. Sugino, Appl. Surf. Sci. **85**, 239 (1995); T. Akiyama, A. Oshiyama, and O. Sugino, J. Phys. Soc. Jpn. **67**, 4110 (1998).
[5] B. T. Kelly, *Physics of Graphite* (Applied Science, London, 1981).
[6] M. S. Dresselhaus, G. Dresselhaus, and P. C. Eklund, *Science of Fullerenes and Carbon Nanotubes* (Academic, San Diego, 1996).
[7] *Positron Spectroscopy of Solids*, edited by A. Dupasquier and A. P. Mills, Jr. (IOS Press, Amsterdam, 1995).
[8] M. J. Puska and R. M. Nieminen, Rev. Mod. Phys. **66**, 841 (1994).
[9] M. J. Puska, A. P. Seitsonen, and R. M. Nieminen, Phys. Rev. B **52**, 10 947 (1995).
[10] P. Asoka-Kumar *et al.*, Phys. Rev. Lett. **77**, 2097 (1996).
[11] Z. Tang *et al.*, Phys. Rev. Lett. **78**, 2236 (1997); Z. Tang *et al.*, Phys. Rev. B **57**, 12 219 (1998).
[12] M. Hasegawa *et al.*, Mater. Sci. Forum **105–110**, 1041 (1992).
[13] S. Berko, R. E. Kelley, and J. S. Plaskett, Phys. Rev. **106**, 824 (1957).
[14] M. Shimotomai *et al.*, J. Phys. Soc. Jpn. **52**, 694 (1983).
[15] P. Hautojärvi and C. Corbel, in *Positron Spectroscopy of Solids* (Ref. [7]), p. 491.
[16] D. J. Chadi and M. L. Cohen, Phys. Rev. B **8**, 5747 (1973).
[17] The calculated lifetime for the V_9 (C_{3v}) using a 128-site supercell and a maximum kinetic energy of 700 eV agrees with the present value within 2 ps.
[18] The vacancy clusters will be subjected to recombination with interstitials released from interstitial clusters during annealing and then to decrease in their densities, which will give the decrease in I_3 (Table II).